9

Ballistics Image Processing and Analysis for Firearm Identification

Dongguang Li
School of Computer and Security Science
Faculty of Computing, Health and Science
Edith Cowan University
2 Bradford Street, Mount Lawley,
Western Australia 6050

1. Introduction

The identification of firearms from forensic ballistics specimens is an exacting and intensive activity performed by specialists with extensive experience. The introduction of imaging technology to assist the identification process of firearms has enhanced the ability of forensic ballisticians to conduct analyses of these specimens for identification.

The positive identification of ballistics specimens from imaging systems are important applications of technology in criminal investigation [1] [2] [3] [4]. While the image capture methodology for persons and forensic ballistics specimens is similar, the process of identification for each is dependent upon the level of certainty required for the identification.

The forensic identification of ballistics specimens relies on the detection, recognition and ultimate matching of markings on the surfaces of cartridges and projectiles made by the firearms [5]. Traditional methods for the comparison of these marks are based on incident light microscopy. The image formed from the oblique illumination of the mark gives a representation of the surface of the specimen in the region of the mark [6]. This representation is critically dependent on the material of the surface on which the marks have been made, and the geometry and intensity of the illumination system. The assessment by the ballistician of the similarity between comparable marks on respective ballistics specimens from crime scenes and test firings will be based on the expertise and experience of the technologist. Thus the traditional method of matching markings has inherent difficulties, and entails an element of subjectivity [7].

The need for firearm identification systems by police services continues to increase with greater accessibility to weapons in the international contexts. The characteristic markings on the cartridge and projectile of a bullet fired from a gun can be recognized as a *fingerprint* for identification of the firearm [8]. Forensic ballistics imaging has the capacity to produce high-resolution digital images of cartridge cases and projectiles for matching to a library of ballistics images [9]. However, the reliance upon imaging technologies makes identification of ballistics specimens both a demanding and exacting task, where the control of the error of

Source: Image Processing, Book edited by: Yung-Sheng Chen,
ISBN 978-953-307-026-1, pp. 572, December 2009, INTECH, Croatia, downloaded from SCIYO.COM

measurement in the imaging technique must not allow compromise of integrity of the identification process.

The analysis of marks on bullet casings and projectiles provides a precise tool for identifying the firearm from which a bullet is discharged [1] [10]. The characteristic markings of each cartridge case and projectile are released ready for analysis when the gun is fired. More than thirty different features within these marks can be distinguished, which in combination produce a "fingerprint" for identification of the firearm [11]. This forensic technique has wide application in the world of forensic science, and would play a vital part in legal evidence in the case where firearms are involved.

Projectile bullets fired through the barrel of a gun will exhibit extremely fine striation markings, some of which are derived from minute irregularities in the barrel, produced during the manufacturing process. The examination of these striations on land marks and groove marks of the projectile is difficult using conventional optical microscopy. However, digital imaging techniques have the potential to detect and identify the presence of striations on ballistics specimens.

Given a means of automatically analyzing features within such a firearm "fingerprint", identifying not only the type and model of a firearm, but also each individual weapon as effectively as human fingerprint identification can be achieved. Due to the high demand of skill and the intensive nature of ballistics identification, law enforcement agencies around the world have expressed considerable interest in the application of ballistics imaging identification systems to both greatly reduce the time for identification and to introduce reliability (or repeatability) to the process.

Several ballistics identification systems are already available either in a commercial form or in a beta-testing state. The two major international ballistics imaging systems are manufactured by the IBIS Company in Montreal, Canada and the FBI (Drugfire) in USA. A Canadian company, Walsh Automation, has developed a commercial system called "Bulletproof", which can acquire and store images of projectiles and cartridge cases, and automatically search the image database for particular striations on projectiles. However the user must match the impressed markings or striations on the projectiles. This inherent limitation of the system with respect to projectiles has prohibited its use. The biometric imaging and ballistics imaging expertise at Edith Cowan University (ECU) in Australia have developed the next generation of digital imaging and surface profiling information systems for forensic ballistics identification, for solving weapon related crime in Australia and in the international context. The Fireball Firearm Identification System was developed at ECU after the initial research conducted by Smith [1][9] and Cross [1], and later by an ECU software team [12]. The Fireball System was acknowledged as the leading small ballistics identification system in the world [13]. The Fireball has the capability of storing and retrieving images of cartridge case heads, and of interactively obtaining position metrics for the firing-pin impression, ejector mark, and extractor mark. The limitation of this system is that the position and shape of the impression images must be traced manually by the user. For the time being, we still have unsolved problems on projectiles imaging, storing and analyzing although the system has been put in use for nine years already. The efficiency and accuracy of the FireBall system must be improved and increased.

The research papers on the automatic identification of cartridge cases and projectiles are hardly found. L.P. Xin [14] proposed a cartridge case based identification system for firearm authentication. His work was focused on the cartridge cases of center-firing mechanisms.

And he also provided a decision strategy by which the high recognition rate would be achieved interactively. C. Kou et al. [15] described a neural network based model for the identification of chambering marks on cartridge cases. But no experimental results were given in their paper. Using a hierarchical neural network model, a system for identifying the firing pin marks of cartridge cases images automatically is proposed in this paper. We mainly focus on the consideration of rim-firing pin mark identification. A significant contribution towards the efficient and precise identification of cartridge cases in the further processing, such as the locating and coding of ejector marks, extractor marks and chambering marks of cartridge cases will be made through this system. The SOFM neural network and the methods of image processing in our study is described briefly in Section 4.
The identification of the ballistics specimen from the crime scene with the test specimen is traditionally conducted by mapping the marks by visual images from a low-powered optical microscope (Fig. 1). The selection of features within the identifying mark is chosen for their apparent uniqueness in an attempt to match both crime scene and test specimens. A decision is made whether the same firearm was responsible for making the marks under examination on the crime scene and test ballistics specimens. The selection of the mark or set of marks for examination and comparison is a critical step in the identification process, and has the capacity to influence subsequent stages in the comparison process [2].

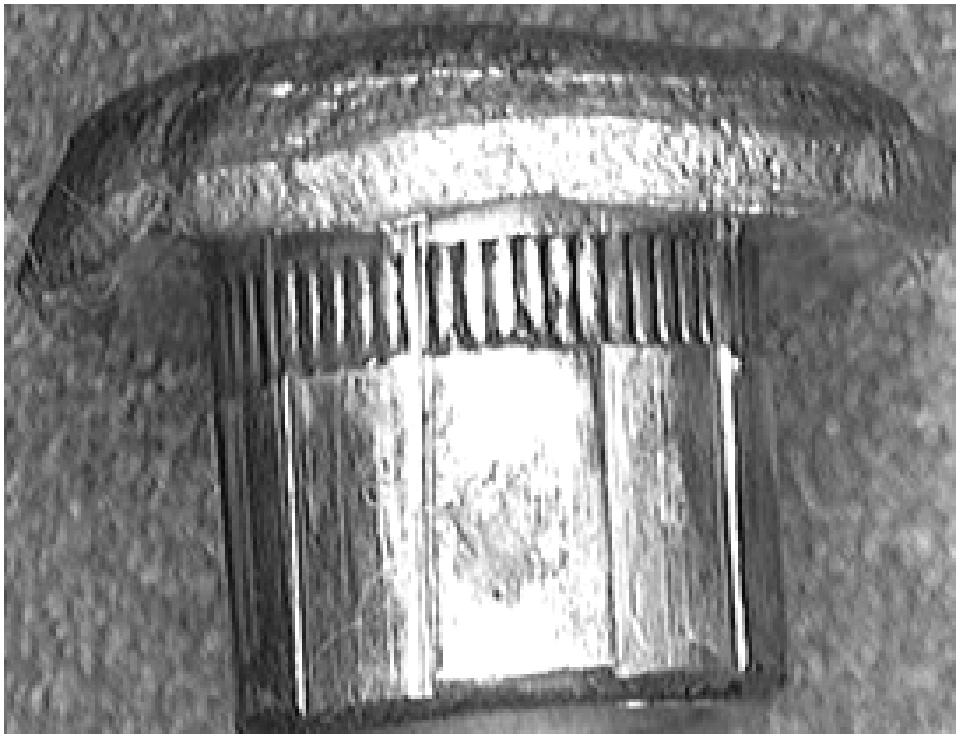

Fig. 1. Landmarks and groove marks of a fired projectile

However, optical and photonic techniques have the capability of a quantum improvement in quality of images for comparison, and as a result will enhance reliability and validity of

the measurements for matching images. The line-scan imaging (Fig. 2) and profilometry techniques [2] [3] each contribute to the information base that will allow identification of firearms from matching crime scene and test fired ballistics specimens.

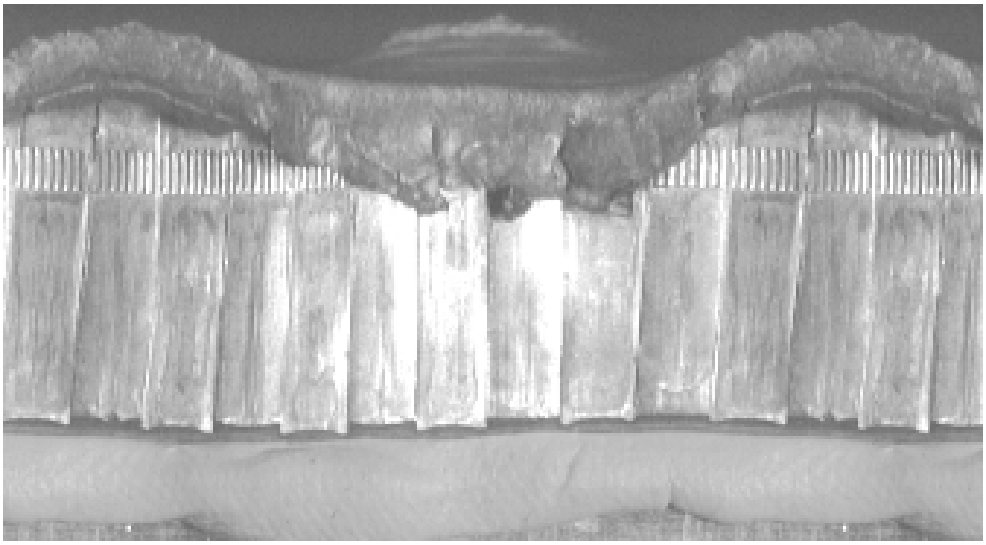

Fig. 2. Linescan image of fired projectile

The development of the line-scan technique [2] [16] [17] for ballistics specimens has the capacity to produce images for the spatial distribution of identification signatures on cylindrical projectiles and cartridge cases. This is achieved by maintaining the surface of the specimen at focus for the rotational scan of the cylinder. However, the production of high resolution images of the cylindrical ballistics specimens are still required for comparison and hence identification.

The difficulties associated with traditional imaging of forensic ballistics specimens are numerous, and include the smallness of the samples, the nature of the surfaces for the cartridge cases (brass) and for the projectiles (lead). As well the features used for identification have low contrast, the cylindrical shape of the cartridge cases, and the distorted shapes of the projectiles (after striking objects) all causing focus problems for image formation.

In this chapter, a new analytic system based on the Fast Fourier Transform (FFT) for identifying the projectile specimens captured by the line-scan imaging technique is proposed. The system gives an approach for projectiles capturing, storing and automatic analysis and makes a significant contribution towards the efficient and precise identification of projectiles. Firstly, in Section 2, the line-scan imaging technique for projectile capturing is described. Secondly, the analytic approach based on FFT for identifying the projectile characteristics and the experimental results are presented in Section 3. The artificial intelligent techonologies are applied to the ballistics image classification and identification in Section 4. In Section 5, the image database systems are discussed in details. Some online image procissing and visualizition applications are covered in Section 6. Finally, suggestions on the further research and conclusion are given in Section 7.

2. Line-scan imaging technique for projectile capturing

The proposed analysis system for identifying firearms based on the projectiles images is composed of three parts (shown in Fig. 3), and each part is described in detail in following sections.

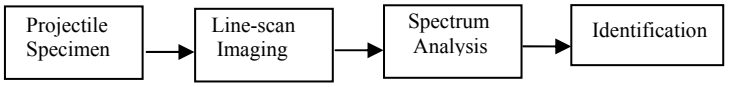

Fig. 3. The proposed analysis system for firearm identification based on projectiles

2.1 Line-scan Imaging

Due to the expected high contrast imaging involved in imaging the cylindrical shapes of ballistics specimens, the traditional optical microscopy technique is inherently unsuitable. As the specimen is translated and rotated [17], it is difficult to maintain image quality using oblique lighting on a cylindrical surface at low magnification microscopy. However, in order to obtain the surface information from a cylindrical shaped surface, a line-scan imaging technique is used by scanning consecutive columns of picture information and storing the data in a frame buffer so that a 2D image of the surface of the cylindrical specimen is produced.

The precursor-imaging device to the line-scan camera is the periphery camera, which consists of a slit camera with moving film in order to 'unwrap' cylindrical objects by rotating them on a turntable [18]. Relative motion between the line array of sensors in the line-scan camera and the surface being inspected is the feature of the line-scan technique. To achieve this relative motion, the cylindrical ballistics specimen relative to the stationary line array sensors are rotated [17][18][19][20].

Due to the line-scan technique, all points on the imaging line of the sample are in focus. This is because the cylindrical ballistics specimen is rotated about an axis of rotation relative to a stationary line array of sensor. Thus, during one full rotation of the cylindrical ballistics specimen, all points on the rotating surface will be captured on the collated image. [17].

The line-scan imaging analysis system for projectiles in our study is shown in Fig. 4. The stepper motor rotates with 360 degrees/ 2400 steps, namely 0.15 degree each step. The 0.15 degree stepper motor is used in order to acquire sufficient details from the surface of the projectile. For example, a projectile with a diameter of 5-15mm has a perimeter range of 15-50mm roughly. With 2400 steps a round the lowest resolution of the line-scan image will still be 2400/ 50=48 lines per mm. A CCD camera (Sony, Model DXC-151AP) is used instead of the traditional camera used in [17] [18]. The graphic capturing card installed in the PC has an image size of 320× 240 pixels. A ring light source (Leica 30120202) is adopted, which can provide uniform lighting conditions [21]. The optical system used was just a standard optical microscope (Leica MZ6).

Being quite different from the method used in [17] [18], the procedure in our line-scan imaging approach is as follows:

1. With the stepper motor's every step
2. the CCD camera captures the current image of projectile specimen and
3. sends the image to Graphic card in PC;
4. The middle column of pixels in this image is extracted and saved consecutively in an array in the buffer on PC, and

5. steps 1. and 2. are repeated until the whole surface of the projectile specimen is scanned;
6. The array in the buffer is used to produce a 2-D line-scanned image for the whole surface of the projectile.

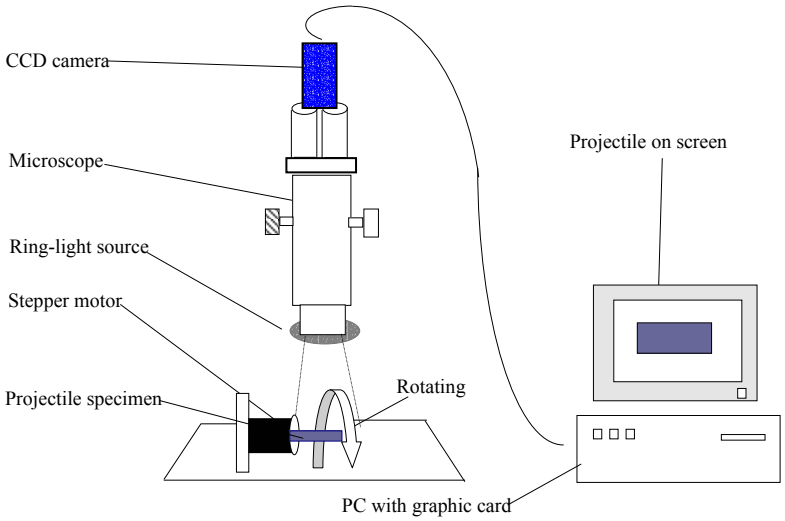

Fig. 4. The line-scan imaging and analyzing system

The resolution of the line-scan image is dependent on,

- the rotational degree per step of the stepper motor
- the resolution of CCD camera
- the resolution of graphic capturing card
- the columns captured at each step in step

By adjusting the length of each step of the stepper motor and the number of columns captured in each step to meet forensic investigation requirements, the resolution of the line-scanned image of projectile specimen could be manipulated. The resolution required to detect the major striations on land marks and groove marks is not necessary to be very high. The line-scan image resolution is set by the rotational steps and sizes of the projectile specimen.

2.2 Projectile specimens and their line-scanned images

The projectile specimens in our study, provided by Western Australia Police Department, are in four classes and belong to four different guns. They are:

1. Browning, semiautomatic pistol, caliber 9mm.
2. Norinco, semiautomatic pistol, caliber 9mm.
3. and 4. Long Rifle, semiautomatic pistol, caliber 22 (5.59mm).

Through the use of the line scan imaging technique as discussed in Section 2.1, all the projectile specimens in our study are recorded under the same conditions (e.g light conditions, the stepping angle of the stepper motor etc…). All the landmarks and groove marks of projectile specimen are captured and displayed in the line scanned image through adjusting the stepping angle of the stepper motor by just one full rotation (360 degrees).

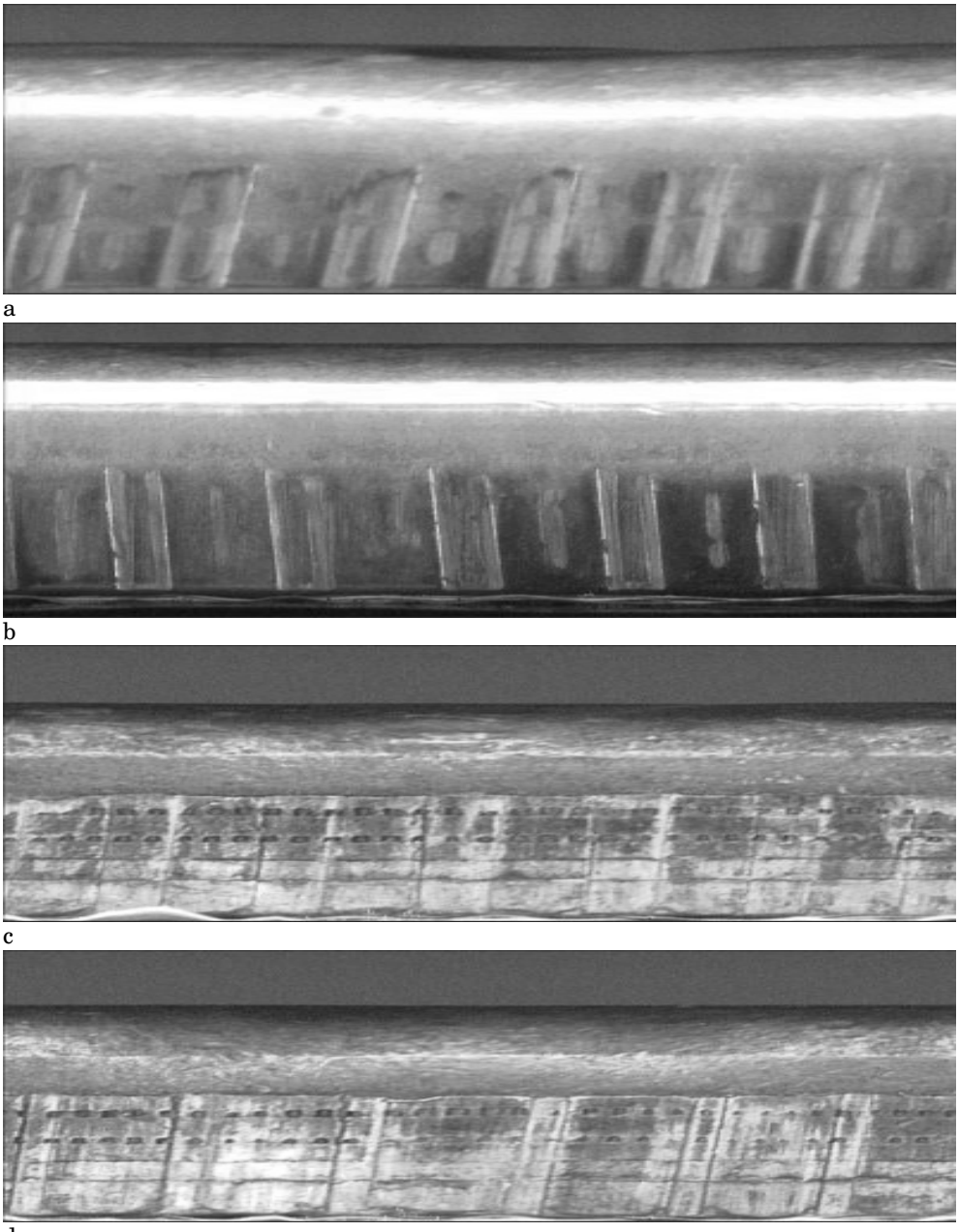

Fig. 5. Four classes of line-scanned images of projectiles in our study (with code: a, 101; b, 201; c, 301; d, 401)

Line-scanned images of four classes of projectile specimens in our study are shown Fig. 5. For the purpose of firearm identification, what we are looking at in these images are some unique features such as land mark width, groove mark width, and their orientations. Obviously there are many more different features (visible or hidden) in the different images. All those features form a unique combination for each every weapon as a set of fingerprints for that particular weapon.

2.3 Image pre-processing for FFT analysis

In a practical application, the quality of the line-scanned image of a projectile specimen can be affected and noised by many factors such as the lighting conditions, the materials of the specimen, the original texture on the surface of specimen, and the deformed shapes. Strong noise and damage in the line-scanned image may result, and this would mean difficulties in extracting and verifying the important features used for identifying the individual specimen, such as the contours, edges, the directions and the width (or distance) of land marks and groove marks. To eradicate or minimize the effects mentioned above, the following image pre-processing operations are applied to the line-scanned images obtained in Section 2.2.

A general function of image preprocessing is the contrast enhancement transformation [22]. Low-contrast images can be a result of poor lighting conditions, lack of dynamic range of the imaging sensor, and a wrong setting of lens aperture during image acquisition. Increasing the dynamic range of gray levels in the image being processed is the idea behind contrast enhancement. In our study, the images are often blurred to a certain extent due to the reason of the strong reflection from the metal surface. The landmarks or groove marks may be hidden within. Thus, the contrast enhancement transformation is used upon the images obtained in Section 2.2. We perform a simple contrast enhancement by linearly expanding the contrast range by assigning the darkest pixel value to black, the brightest value to white, and each of others to linearly interpolated shades of grey in the image. The operation is automated when acquiring the images with a CCD camera. In the line-scanned images, only the regions that include the landmarks and groove marks are useful for analyzing and identifying the characteristics of the projectile specimens. Thus, we only select the regions in images that are necessary and useful to our study. The images (the effective regions in original images) shown in Fig. 6 are transformed versions corresponding to the images in Fig. 5 by the region selecting and the contrast enhancement transformation.

One of the most important roles in the identification system is feature extraction. There are many ways to perform edge detection. However, the most may be grouped into two categories, Gradient and Laplacian. The gradient method detects the edges by looking for the maximum and minimum in the first derivative of the image. The Laplacian method searches for zero-crossings in the second derivative of the image to find edges. For detection of edge and lines in our line-scan images of projectiles, various detection operators can be used. Most of these are applied with convolution masks and most of these are based on differential operations. We pick up the first derivatives [22] as the images features. For a digital image, Sobel operators in vertical and horizontal directions (shown in Fig. 7 with 3×3 window) are the most popular powerful masks used to approximate the gradient of f at coordinate (i, j). In our experiments, we adopt the Sobel operators to extract the contours and edges of the land and groove marks on line-scanned images of projectile specimens, which convolves the images with the Sobel masks to produce the edge maps of the four line-scan images shown in Fig. 8. Because the directions of the land and the groove marks of the projectile specimens are mostly along 90 degrees in the line-scanned images,

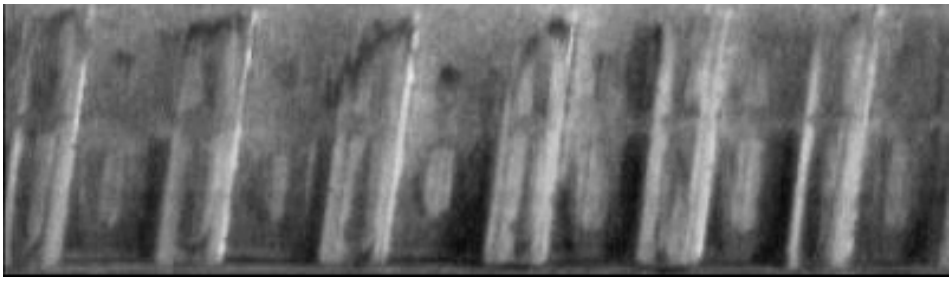

a

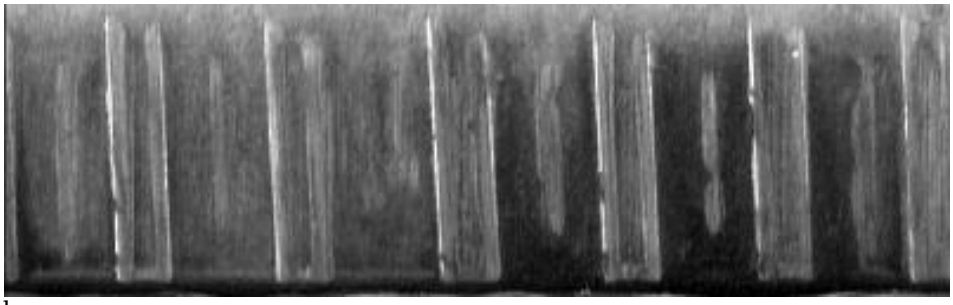

b

c

d

Fig. 6. Contrast enhancement results (a, b with size 400× 110, and c, d with size 400× 100)

-1	-2	-1		-1	0	1
0	0	0		-2	0	2
1	2	3		-1	0	3

Fig. 7. Sobel masks in vertical and horizontal directions

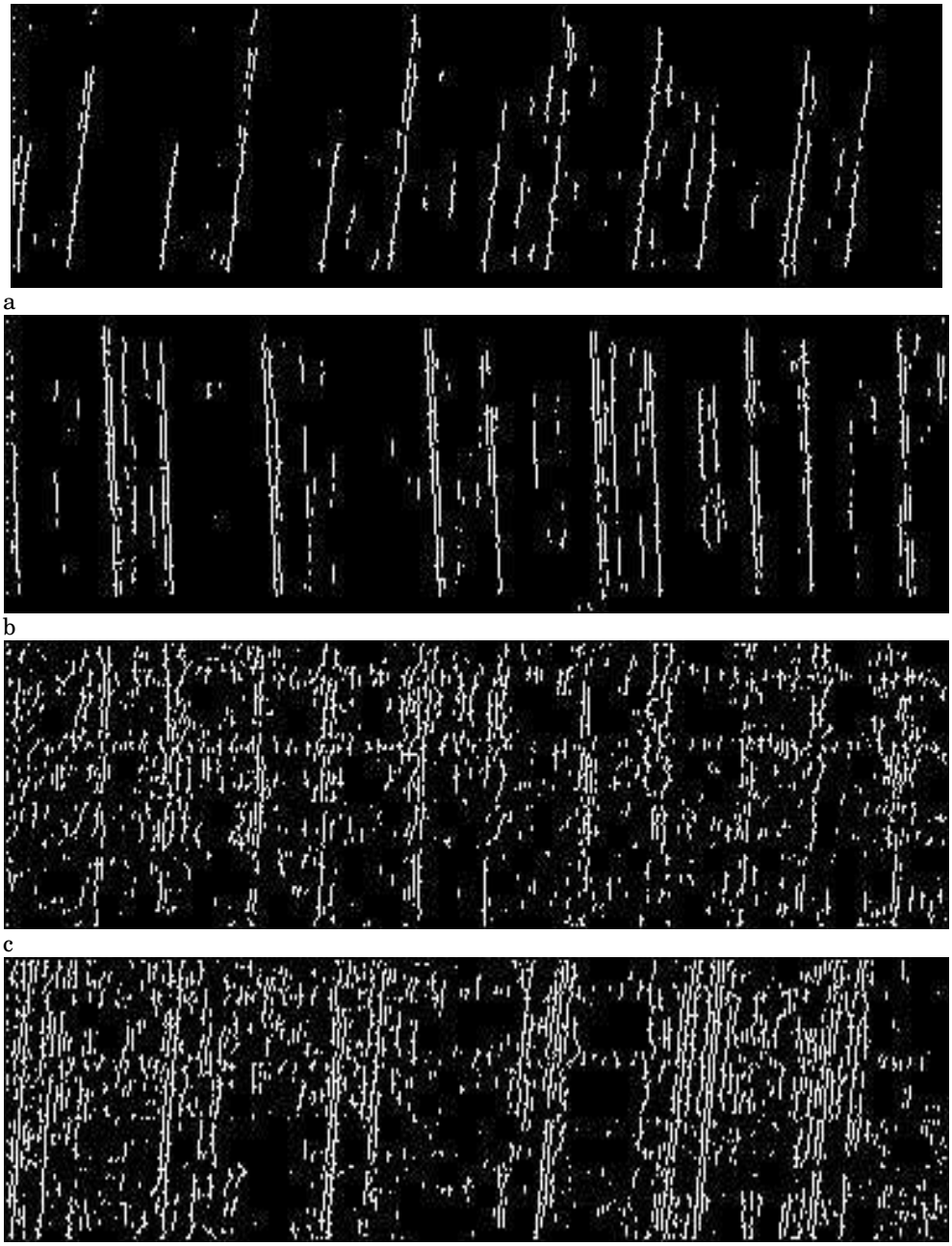

a

b

c

d

Fig. 8. The contours and edges extracting using Sobel operator in vertical direction

we only adopt the vertical direction mask (Fig. 7) for extracting the features of the line-scanned images. Through an observation of Fig. 8 in which there are lots of noises and disconnection on the land and groove marks, the conventional spatial techniques are not suitable for the nature of locally. Hence, a FFT-based analysis for projectiles is introduced.

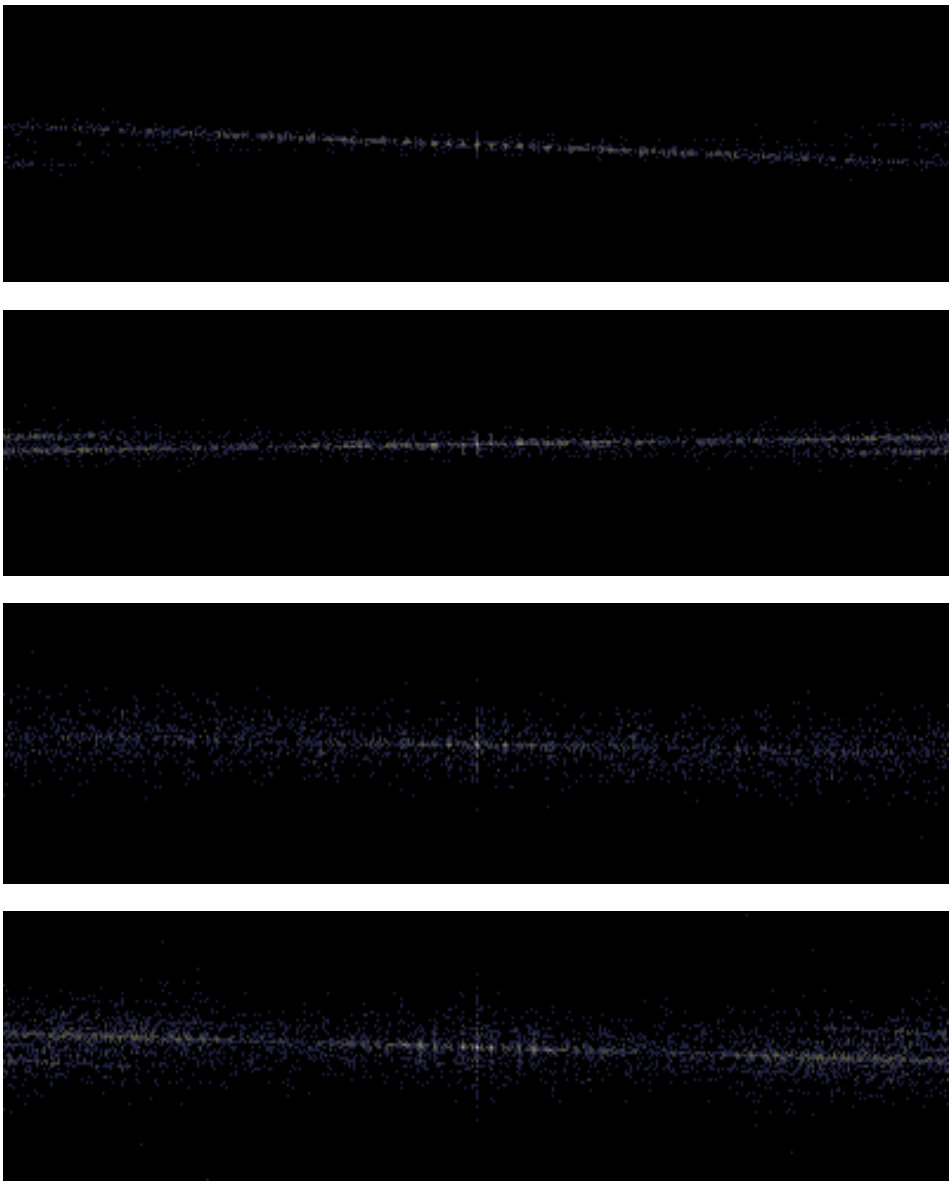

Fig. 9. Fourier transformation results of the images in Fig. 8

3. FFT-based analysis

3.1 FFT and spectrum analysis

The Fourier transform of a two-dimensional, discrete function (image), $f(x,y)$, of size $M \times N$, is given by the equation

$$F(u,v) = \frac{1}{MN} \sum_{x=0}^{M-1} \sum_{y=0}^{N-1} f(x,y) e^{-j2\pi(ux/M + vy/N)} \tag{1}$$

where $j = \sqrt{-1}$, for all $u = 0, 1, 2, \cdots, M-1$, $v = 0, 1, 2, \cdots, N-1$. We define the Fourier spectrum by the equation

$$| F(u,v) | = \left[R^2(u,v) + I^2(u,v) \right]^{1/2} \tag{2}$$

where $R(u,v)$ and $I(u,v)$ are the real and imaginary parts of $F(u,v)$, respectively.

For describing the directionality of periodic or almost periodic 2-D patterns in an image, the Fourier spectrum is ideal. As easily distinguishable as concentrations of high-energy burst in the spectrum, these global texture patterns are generally not convenient to detect with spatial methods because of the local nature of these techniques. In the feature extraction process some of texture descriptors are considered both in Fourier and spatial domains. It is noticed that some of spatial domain descriptors can be used with success for geology recordings where the image appears to be very similar to the one in this research [23].

For the specific research interests in this study we only consider a set of features of the Fourier spectrum that are used for analyzing and describing the line-scanned images of projectiles:

1. Principal direction of the texture patterns are shown by prominent peaks in the spectrum.
2. Fundamental spatial period of the patterns are shown by the location of the peaks in the frequency plane.
3. Some statistical features of the spectrum.

By expressing the spectrum in polar coordinates to yield a function $S(r,\theta)$, where S is the spectrum function, and r and θ are the variables in this coordinate system, detection and interpretation of the spectrum features just mentioned often are simplified. For each direction θ, $S(r,\theta)$ is a 1-D function $S_\theta(r)$. Similarly, for each frequency r, $S_r(\theta)$ is a 1-D function. Analyzing $S_\theta(r)$ for a fixed value of θ yields the behavior of the spectrum (such as the presence of peaks) along a radial direction from the origin, whereas analyzing $S_r(\theta)$ for a fixed value of r yields the behavior along a circle centered on the origin. A more global description is obtained by integrating (summing for discrete variables) these functions [22]:

$$S(r) = \sum_{\theta=0}^{\pi} S_\theta(r) \tag{3}$$

and

$$S(\theta) = \sum_{r=1}^{R_0} S_r(\theta) \tag{4}$$

where R_0 is the radius of a circle centered at origin.

The results of Equations (3) and (4) constitute a pair of values $[S(r), S(\theta)]$ for each pair of coordinates (r, θ). We can generate two 1-D functions, $S(r)$ and $S(\theta)$, that constitute a spectral-energy description of texture for an entire image or region under consideration by varying these coordinates. Furthermore, descriptors of these functions themselves can be computed in order to characterize their behavior quantitatively, which can be used as ballistics features for firearm identification.

3.2 FFT-based analysis, identification and experimental results

The following section discusses in detail some characteristics and descriptors of the line-scanned images for identification of projectiles using the radius spectrum and angular spectrum.

We know that the slowest varying frequency component ($u = v = 0$) corresponds to the average gray level of an image. The low frequencies correspond to the slowly varying components of an image as we move away from the origin of the transform. In a line-scanned image of projectile specimen, for example, these might correspond to the land and groove marks which are large in scale and regular in shape. Moving further away from the starting point, the higher frequencies begin to correspond to faster and faster gray level changes in the image. These are the small or irregular marks and other components of an image characterized by abrupt changes in gray level, such as noises. Now we focus our attention on the analysis of low frequencies in the radius and angle spectrum of line-scanned images.

Shown in Fig. 10 a, b, c and d, are the plots of radius and angle spectrum corresponding to images in Fig. 9 a, b respectively. The results of FFT clearly exhibit directional 'energy' distributions of the surface texture between class one and two. Comparing Fig. 10 a to b, the plots on the radius spectrum, six clear peaks in the range of low frequencies (r <20) can be observed on the former whilst the latter has only three peaks in the same range and is smooth in shape, this indicates that 'energy' of the class one specimen is distributed in several permanent positions, and also reveals that the class one specimen has a coarse surface texture and the wide land and groove marks, while the surface texture of class two is fine and the smaller widths of land and groove marks.

The angular spectrums (Fig. 10 c and d) display a great distinctness in position of prominent peaks between class one and two. With respect to the measurement coordinate, further study reveals that the angular spectrum can clearly indicate the angular position of periodic grooves or scratches on the surface. It can be seen from the angular spectrum there is a maximum peak at about 81 degrees in Fig. 10 c. This is indicative of scratches (the land or groove marks) oriented 81 degrees to the surface of the projectiles, while the maximum peak in Fig. 10 d sits at about 95 degree. Furthermore, a second prominent peak of about 100 degrees (corresponding to small or shallow marks on the projectile's surface) can be seen on the former plot. However, it is noted that the second peak of Fig. 10 d is at about 85 degree.

By examining quantitative differences of spectrums using a set of features, the characteristics of projectile specimen surface textures can also be revealed.

To compare and analyze the spectrum differences between the two classes easily, a set of features is used, and the quantitative results are shown in Table 1 (where, r_1 and a_2, Max; r_2 and a_3, Mean; r_3 and a_4, Std; r_4 and a_5, Max: Median; and a_1, Position of maximum peak).

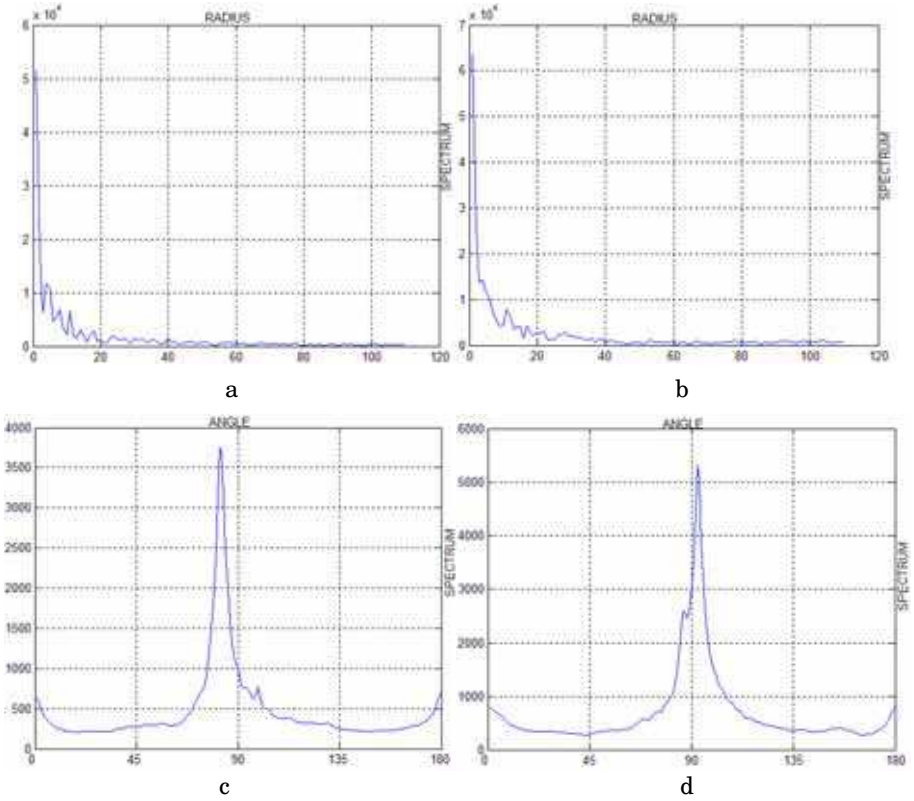

Fig. 10. Radial spectrum (a, b) and Angular spectrum (c, d) of the images (a, b) in Fig. 9

As observed from Table 1, the Max, Mean, and Std of class one are relatively smaller than class two, while the relative variation for radio between Max and Mean is greater. The difference between prominent peaks (corresponding to the orientations of land and groove marks) of class one and two is 14 degrees. All this goes to show that FFT spectrum analysis, in the form of quantification, can reveal characteristic and directional surface textures of the projectile specimen.

Class	Code	Radial spectrum				Angular spectrum				
		r_1	r_2	r_3	r_4	a_1	a_2	a_3	a_4	a_5
1	101	51517	1728	5372	29.81	81	3753	475.2	546.2	7.898
2	201	63646	2538	6809	25.07	95	5308	697.9	794.7	7.600

Table 1. Radial spectrum and angular spectrum statistics results of Fig. 9 a and b

After obtaining the initial significant results, the 12 more experiments involving 12 new projectile specimens fired by 12 different weapons are carried out. Those 12 specimens are among the four classes of weapons discussed in the section 2.2 and coded in Fig. 5 (4 in class 1, code 102-105; 2 in class 2, code 202-203; 3 in class 3, code 302-304; and 3 in class 4, code 402-404). Table 2 lists all the experimental results based on the total 16 projectile specimens in our study.

Class	Code	Radial spectrum				Angular spectrum				
		r_1	r_2	r_3	r_4	a_1	a_2	a_3	a_4	a_5
1	101	51517	1728	5372	29.81	81	3753	475.2	546.2	7.898
	102	51162	1591	5187	32.16	81	3709	437.6	545.6	8.487
	103	51200	1520	5087	33.68	81	3583	418.2	509.8	8.571
	104	51556	1699	5348	30.34	81	3589	467.3	514.1	7.685
	105	62715	1962	6299	31.96	81	4219	539.5	617.8	7.827
2	201	63646	2538	6809	25.07	95	5308	697.9	794.7	7.600
	202	64381	2738	7038	23.51	95	5257	752.9	777.7	6.990
	203	64059	2545	6707	25.16	95	5193	700.0	794.0	7.419
3	301	63959	2899	6942	22.06	86	2514	724.7	451.9	3.469
	302	64448	2478	6889	26.01	86	2714	719.4	445.5	3.774
	303	64288	2743	7090	23.43	86	2517	685.8	439.9	3.669
	304	63694	3011	6999	21.23	86	2750	752.7	512.8	3.657
4	401	76059	4040	8554	18.27	79	4965	1010	787.8	4.916
	402	76406	5026	8982	15.20	79	4972	1256	835.6	3.959
	403	75607	3735	8035	20.23	79	4897	933.9	753.3	5.249
	404	76796	3786	8498	20.28	79	4135	946.3	738.6	4.371

Table 2. Radial spectrum and angular spectrum statistics results based on the specimens in our study

By observing Table 2 and recalling that the calibers of class one and two are the same, and so are the class three and fours, we can easily identify the projectiles into a class using the features listed in Table 2. For example, all the values of r_4 for class one are greater than 28.0, while for class two, none is greater than 26.0. In order to identify the firearms to the level of the single gun we treat each every row of the table 2 as a set of fingerprints from that gun. The characteristics (r_1-r_4 and a_1- a_5) we used in spectrum analysis can be formed as a set of features vectors for building an artificial intelligent (AI) system for the automatic firearm identification based on the spent projectiles. Several AI algorithms are under investigation to best use the spectrum characteristics as searching criteria in the existing FireBall firearm identification database.

4. SOFM and cartridge case image processing

It is hard to find research papers on the automatic identification of cartridge. A cartridge cases based identification system for firearm authentication was proposed by Le-Ping Xin [14]. His work was focused on the cartridge cases of center-fire mechanism. And he also provided a decision strategy from which the high recognition rate would be achieved interactively. A neural network based model for the identification of the chambering marks on cartridge cases was described by Chenyuan Kou et al. [24]. But no experiment results were given in their paper.

In this section a proposed hierarchical firearm identification model based on cartridge cases images is shown. The following parts, describe respectively, the structure of the model, the training, testing of SOFM, and decision-making strategy.

4.1 SOFM neural network

The basic classifying units in our identification system is picked as the Self-Organizing Feature Map (SOFM) neural networks. The SOFM has been applied to the study of complex problems such as speech recognition, combinatorial optimization, control, pattern recognition and modeling of the structure of the visual cortex [25], [26], [27] and [28]. The SOFM we used is a kind of un-supervised neural network models, it in effect depicts the result of a vector quantization algorithm that places a number of reference or codebook vectors into a high-dimension input data space to approximate defined values between the reference vectors, the relative values of the latter are made to depend on it to its data set in an ordered fashion. When local-order relations are each other as if there neighboring values would lies along an "elastic surface". This "surface" becomes defined as a kind of nonlinear regression of the reference vectors through the data points [29], by means of the self-organizing algorithm.

We employ the standard Kohonen's SOFM algorithm summarized in Table 3, the topology of SOFM is shown in Fig. 11.

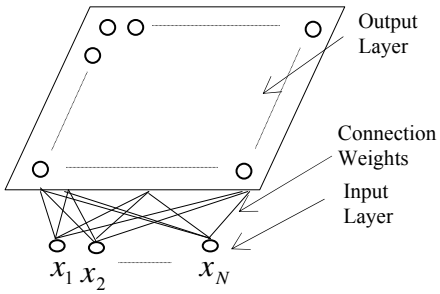

Fig. 11. The topology of SOFM

4.1.1 Identification model

The system proposed comprises of three stages as shown in Fig. 12, the preprocessing stage as mentioned in Section 2 and Section 3, the classification stage based on neural networks involving two levels SOFM neural networks and the decision-making stage. In our study, the two levels SOFM neural networks are:

The first level has one SOFM neural network (as shown in Fig. 11) labeled by $SOFM_0$ which acts as a coarse classifier among the training (or testing) patterns presented to it. The training or learning processing is the same as that mentioned in Section 4.1.2, which belongs to the unsupervised learning type.

Comprising several child SOFM networks denoted by $\mathrm{SOFM}_i \quad i = 1, 2, \cdots, n$, where n is the number of child SOFM networks is the second level of neural networks, making fine identification among the patterns classified by SOFM_0 (or the output of SOFM_0).

4.1.2 Training

In our study, The training or learning processing for $SOFM_0$ is identical to that mentioned in Table 3, which belongs to the type of unsupervised learning (we use the images of C to train the $SOFM_0$. The number of neurons in input layer is 48×196, corresponding to the size of

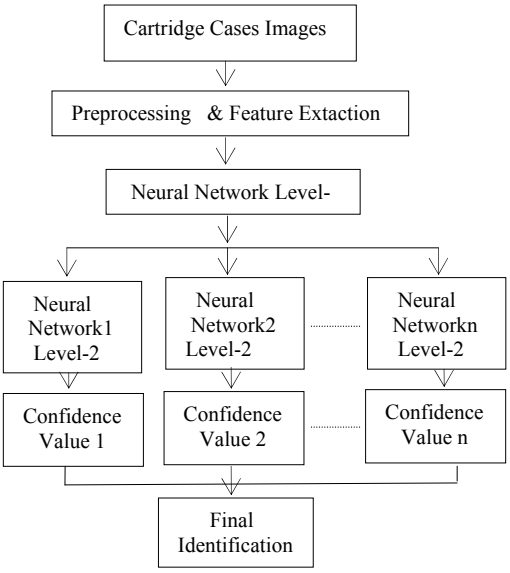

Fig. 12. The proposed identification system

windows normalized (as mentioned before). In the training phase, when a neuron of output layer is inactive for a period of time, it is removed from the network. If a neuron is not chosen frequently as the winner over a finite time interval, it may be considered inactive. After being trained, the neurons, which are active with high output value in the output layer of $SOFM_0$, stand for the classes to which the training images (or the testing specimens) belong. Due to the result of classification of $SOFM_0$ in our study, the training set C has been parted into several subsets. Combination of these subsets in a proper manner achieve training sets for the SOFMs at the second level. When the positions of two classes in the output layer are very close or overlapping the second level SOFM neural networks are generated. The training sets are formed by combining the twoclass patterns for those that are close or overlapping. This training process is identical to that of $SOFM_0$.

4.1.3 Testing

The testing procedure for firearm identification system is as follows:

Step 1. Using a selected testing cartridge case image from the testing set T, present this testing pattern to the first stage of the identification system--the preprocessing stage.

Step 2. Select a type of window from all types in turn, and move this window over the testing pattern processed in Step1 at every location by every pixel horizontally and vertically, pick up the sub-images.

Step 3. Using Formula (5) calculated the confidence values for each sub-image, to do this, present all the sub-images to the $SOFM_0$ in turn, and then to $SOFM_i$ by the result of $SOFM_0$. Return Step2 until all type windows are used up.

Step 4. These confident values are presented to the third stage which is the decision making stage, and using Formula (6) and (7), the final result for the testing cartridge case image is calculated.

4.1.4 Decision-making strategy

For the reasons of noise, lighting conditions, and the trademarks on the head of cartridge cases images, the following situation could generally be encountered in the testing phase:

a. For a testing cartridge case image, when a type of detecting window is used over the image, more than one sub-image under this type window is classified to include a firing pin mark.
b. For a particular testing cartridge case image, when all types of windows are used over the pattern, more than one sub-image under the different windows is classified to include a type of firing pin mark.

To improve the performance and accuracy, we use a final decision-making mechanism in the decision-making stage to solve these problems mentioned above, defining a Confidence Function $D(i, j)$ for the testing pattern i to the jth class which measures the ratio between the testing pattern distance to the weight vectors and the average distance of training patterns to the weight vectors, as follows:

$$D(i, j) = D(j) / D(i, j), \tag{5}$$

where $dist(j)$ is the average distant when all the training patterns, which belong to the jth class, are tested with the jth type window, $dist(i, j)$ is the distant resulted when the ith testing pattern is tested using the jth type window. Defining a decision-making rule as follows: $i \in \text{Class } K$, if

$$D(i,k) = \min_j \{D(i, j) > \Delta_j\}, j = 1, 2, \cdots n, \tag{6}$$

where $\Delta_j \quad j = 1, 2, \cdots n$, is an appropriate threshold selected for the class j by experiments. In General, the unbalance in the neural network for each class results from the unbalanced distribution of training patterns we get in the pattern space. Hence, Δ_j for every class is not unique.

Defining a rejection rule as follows, testing pattern i is rejected by all classes, if

$$D(i, j) < \Delta_j, j = 1, 2, \cdots n, \tag{7}$$

where $\Delta_j \quad j = 1, 2, \cdots n$, is same as in Formula (6).

4.2 Image processing for feature extraction

Contrast Enhancement: The contrast enhancement transformation [30] is one of the general functions in image preprocessing, and function is expressed in Equation (8). Lack of dynamic range in the imaging sensor, or even wrong setting of a lens aperture during image acquisition can all lead to low-contrast images. To increase the dynamic range of the gray levels in the image being processed is the main idea behind contrast enhancement. The image shown in Fig. 13b is transformed by contrast enhancement.

Polar Transaction: Another useful tool in the stage of image preprocessing is polar transformation. In our study, the polar transformation can bring us some advantages: In the test phase, we only move the detecting windows over the testing images in direction of horizontal and vertical rather than rotating the testing images or the detecting windows. This will decrease the numerical error and increase the efficiency. We can get more

informations about the testing images under the Polar systems. Some images that have similar shapes may be different in shapes and be distinguished in Polar Systems.

Step1: Initialize the weights for the given size map. Initialize the learning rate parameter, neighborhood size and set the number of unsupervised learning iterations.

Step2: Present the input feature vector $x = [x_1, x_2, \cdots, x_n, \cdots, x_N]$ in the training data set, where x_n is the n th element in the feature vector.

Step3: Determine the winner node c such that $\|x - w_c\| = \min_i \{\|x - w_i\|\}$

Step4. Update the weights, w_i's, within the neighborhood of node c, $N_c(t)$, using the standard updating rule: $w_i(t+1) = w_i(t) + \alpha(t)[x_n - w_i(t)]$, where $i \in N_c(t)$.

Step5: Update learning rate, $\alpha(t)$, and neighborhood size, $N_c(t)$. $\alpha(t+1) = \alpha(0)\{1 - t/K\}$; $N_i(t+1) = N_i(0)\{1 - t/K\}$, where K is a constant and is usually set to be equal to the total number of iterations in the self-organizing phase.

Step6: Repeat 2-5 for the specified number of unsupervised learning iterations.

Table 3. The Unsupervised SOFM Algorithm

a b c

Fig. 13. Low-contrast image, a. Result of contrast enhancement, b. Result of threshold, c.

$$f(x) = \begin{cases} \frac{y_1}{x_1} x, & x < x_1 \\ \frac{y_2 - y_1}{x_2 - x_1}(x - x_1) + y_1, & x_1 \le x \le x_2 \\ \frac{255 - y_2}{255 - x_2}(x - x_2) + y_2, & x > x_2 \end{cases} . \quad (8)$$

Feature Extracting: Feature extracting plays an important role in recognition system. In the real application, the time consuming feature extracting technique is also a crucial factor to be considered. So we pick up the morphological gradient [30] of the images processed by the two steps mentioned aboved as the images features. We deal with digital image functions of the form $f(x, y)$ and $b(x, y)$, where $f(x, y)$ is the input image and $b(x, y)$ is a structuring element , itself a subimage function.
Gray-scale dilation of f by b, denoted $f \oplus b$, is defined as

$$(f \oplus b)(s,t) = \max\{f(s-x,t-y)+b(x,y) \mid (s-x),(t-y) \in D_f; (x,y) \in D_b\} \quad (9)$$

where D_f and D_b are the domains of f and b, respectively.
Gray-scale erosion of f by b, denoted $f \ominus b$, is defined as

$$(f \ominus b)(s,t) = \min\{f(s+x,t+y)-b(x,y) \mid (s+x),(t+y) \in D_f; (x,y) \in D_b\} \quad (10)$$

where D_f and D_b are the domains of f and b, respectively.
The morphological gradient of an image, denoted g , is defined as

$$g = (f \oplus b) - (f \ominus b). \quad (11)$$

The firing mechanism of the weapon is generally of two types: the firing pin is either rim-firing mechanism or center-firing mechanism, as shown in Fig. 14. The firing pin mark of cartridge case is formed when the bullet is fired. It is one of the most important characteristics for identifying the individual firearm. A variety of firing pins marks have been used in the manufacture of firearms for the rim-firing cartridge cases. In our study, the cartridge cases belonged to six guns can be classified into six types by shape of firing pin marks (shown in Fig. 15).

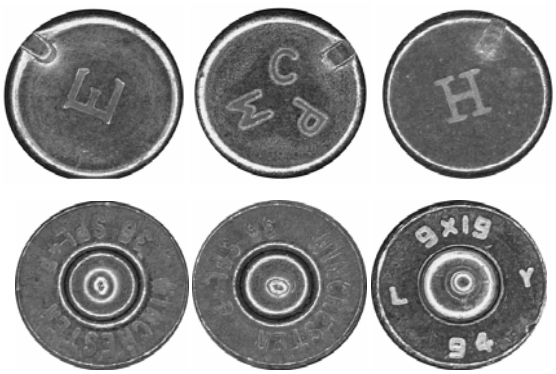

Fig. 14. Rim-firing, first row; Center-firing, second row.

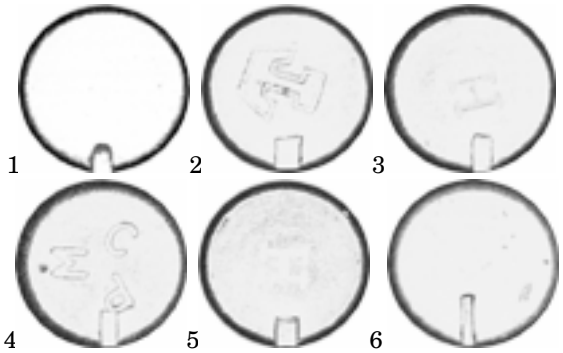

Fig. 15. Six type of cartridge cases images

In the real application, all the images of cartridge cases are obtained through the optical microscope. So some information such as the depth of the impression will be dismissed. Other factors such as the lighting conditions, the material of cartridge cases, and the stamp letters of manufacturer can bring strong noise into the cartridge cases images or damage the shapes of the cartridge cases images. All these would bring many difficulties to feature extracting and identifying. The lighting conditions for the image capturing of cartridge case is crucially importance. In order to produce high contrast of striation (firing-pin mark) on the cartridge cases, the illuminator must be installed at an angle of greater than 45 degree from normal to the plane of the head of the cartridge [1].

The 150 rim-fire cartridge cases, which are belonged to six guns, provided by the Western Australia Police are captured through the optical microscope, one image for each, formed 150 BMP files in gray scale size by 244×240 pixels, and classified into six types by shape of firing pin marks. They are: 1. U-shaped pin mark, 2. Axe-head pin mark, 3. Rectangular (Short) pin mark, 4. Rectangular (Long) pin mark, 5. Square pin mark, 6. Slant pin mark. Examples of the six types are shown in Fig. 15 (The numbers below these figures labeled the class number associated with each cartridge cases). We choose 50 images including the images of all the six guns randomly to form the set C_0 and form the testing set T for the rest images. Then, the images of set C_0 are processed through the image processing and feature extraction stage (shown in Fig. 16) discussed in Section 4.2.

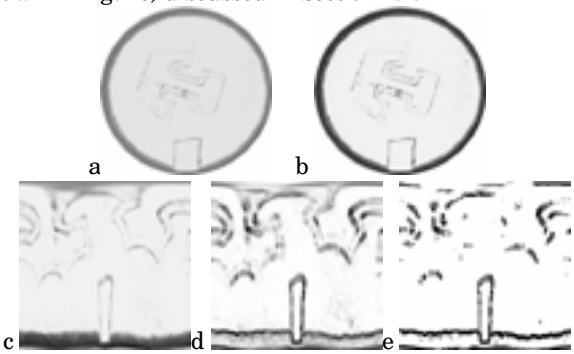

Fig. 16. The original image a, the contrast stretching b, the polar transformation c, the morphological gradient d, the threshold e.

Having been finished the above transformations for the images of every type, we need a "window" operation:

First, windows, size by $n_i \times m_i$ pixels, are used to copy the sub-images---the firing pin marks of the cartridge cases images processed before, where i stands for the label of the class to which the firing pin marks belong. Table 4 shows the sizes of six type windows associated with six type firing pin marks. Second, the images (the firing pin marks) within these six type windows are copied into windows with size normalized by 48×196 pixels to meet the need of having unified input units of SOFM. This process is shown in Fig. 17. To make our model have some robustness to slight variations in the testing cartridge case images, we used the methods as previously described to process a part of our image, we use the following methods: a. Shifted up to two pixels by the direction left, right, up, and down. b. Scaled by factor 0.95 and 0.90. All the images we obtained through the processes mentioned above, along with the number of 350, are combined into a training set C for the model based on SOFM, which will be discussed in the following section.

Type 1	20×96	Type 2	20×96
Type 3	20×120	Type 4	24×116
Type 5	20×120	Type 6	24×168

Table 4. The Size (in pixels) of Six Type Windows

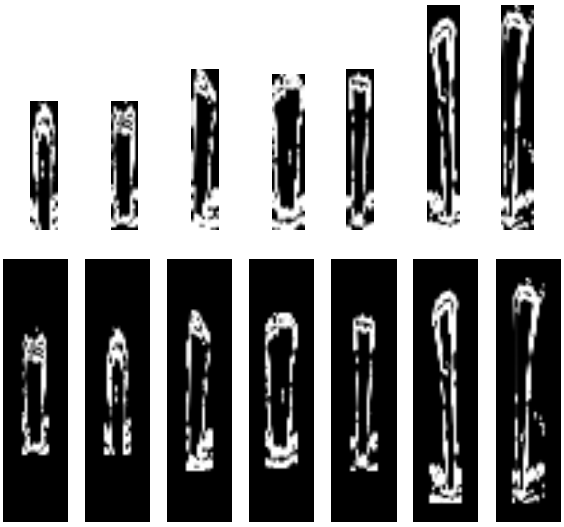

Fig. 17. Six type of firing pin marks within windows with size normalization. The first row shows the six firing pin marks within six type windows. The second row shows the firing pin marks within windows with size normalization.

4.3 Experimental results

In our study, we use the following experimental parameters (shown in Table 5) for $SOFM_0$, Level 2 SOFMs and get experimental results over Training set C.

The neurons of the output layer of $SOFM_0$ are divided into six areas separately, through which the specimens of each class are represented, when the training phase is finished. For the three training sub-networks of the second level, the training set C is divided into three subsets by the fact: the distribution area of each class is not balanced, some classes are near, and others are apart, in following manner:
Subset c_1 including images labeled with class 1 and 2, is selected as the training set of $SOFM_1$,
Subset c_2 including images labeled with class 3 and 5, is selected as the training set of $SOFM_2$,
Subset c_3 including images labeled with class 4 and 6, is selected as the training set of $SOFM_3$.

	Input Layer	Output Layer	$\eta(0)$	$\Lambda_i(0)$
$SOFM_0$	48×196	9×9	0.60	7
$SOFM_1$	48×196	3×3	0.05	2
$SOFM_2$	48×196	5×5	0.05	3
$SOFM_3$	48×196	5×5	0.05	2
	training pattern	right rate	error rate	rejection rate
	350	100%	0%	0%

Table 5. Experimental Parameters for $SOFM_0$, Level 2 SOFMs and Results over Training set C

We have the experiment results over testing set T as follows:

Testing pattern	Right rate
100	97.0%
Rejection rate	Error rate
3.0%	0%

Table 6. Experiments Results

4.3.1 Analysis of experiment results

From the results of Table 6, we can see that the Identification model in our study can make the combination of location and identification of a firing pin mark of a cartridge case images into one stage. It further shows that the model proposed has high performance and robustness for the testing patterns in the following aspects: In the location and identification of firing pin marks: it has high accuracy. Some testing results under Cartesian co-ordinates are shown in Fig. 19. Having robustnesses to the noise patterns, to the damaged and deformed patterns shown in Fig. 19(8-13). Having some robustnesses to the scaled patterns.
For some patterns, we can still see that there are rejections, these rejections are caused mainly by the following reasons: the high noise on the cartridge images; the letters of trademark on the cartridge images; the similitude of one pattern with others in some location.

4.3.2 Further work

In order to improve our model to achieve higher performance, we will do some further research in the following aspects:
In order to improve the quality of image capturing and preprocessing. Another aim of further work would be to extract some fine features with more complex techniques to

represent the patterns (training or testing). Thirdly, it is our aim to integate multiple classifier combination using different feature sets.

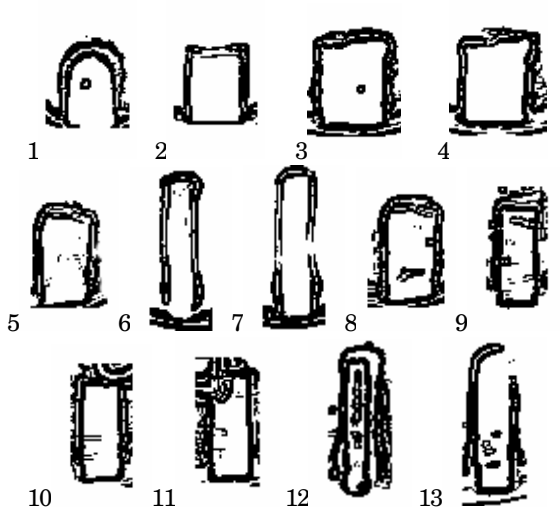

Fig. 19. Some right identification results of testing set T

5. The stand-alone ballistics image database system

A few systems for firearm identification have been developed around world. These includes DRUGFIRE [4], developed by Federal Bureau of Investigation, USA, IBIS[5], developed by Forensic Technology, a division of the Walsh Group, and FIREBALL, developed by Edith Cowan University (ECU) and National Institute of Forensic Science (NIFS) in Australia [1]. These systems integrate digital imaging, database and networking technologies to enhance the capabilities of the forensic firearm examiner.

The FIREBALL firearm identification system is developed as recognizing the need for a low-cost alternative to other established systems. Furthermore, the system is tailored to Australian conditions.

The initial FIREBALL system is a stand-alone system. Each state police department store information in its individual system. Every 3-6 months individual information will be redistributed national wide through CD-ROM. This strategy delays information sharing that is necessary for crime investigation. The stand-alone system also brings the problem for access control and information security.

To overcome shortfalls of the stand-alone system, a web based Fireball is also in progress. The following sections will briefly describe the stand-alone Fireball system and details web applications for querying, visualizing and processing images from Fireball image database on-line.

Fireball is a projectile and cartridge case comparison and image storage database software package developed by Edith Cowan University (ECU), Perth, Australia, and supplied to the National Institute of Forensic Science (NIFS) for the storage of forensic ballistics data by Australian Police Departments. This includes data on firearms, ammunition, fired cartridges cases and projectiles. The system is designed to be a preliminary identification procedure.

Class characteristics of projectile and cartridge cases only are obtained and stored by this system. Class characteristics are gross identifying features that are identical on all cartridge cases and projectiles fired from a particular make and model of firearm (eg. firing pin mark shape).

The information stored in FIREBALL includes data on firearms, ammunition, spent cartridge cases and projectiles. a Graphics User Interface (GUI) is incorporated in FIREBALL, which allows the user to obtain precise ballistics metrics of cartridge case class characteristics (ie. firing pin mark, extractor mark and ejector mark positions) by a simple point-and-click method using the mouse and an on-screen digital image of the head of the cartridge case. Once the class characteristics have been obtained, a search of the database will provide a hit list of corresponding firearms. The system is offered as a preliminary identification procedure, as the technique involves identification by class characteristics

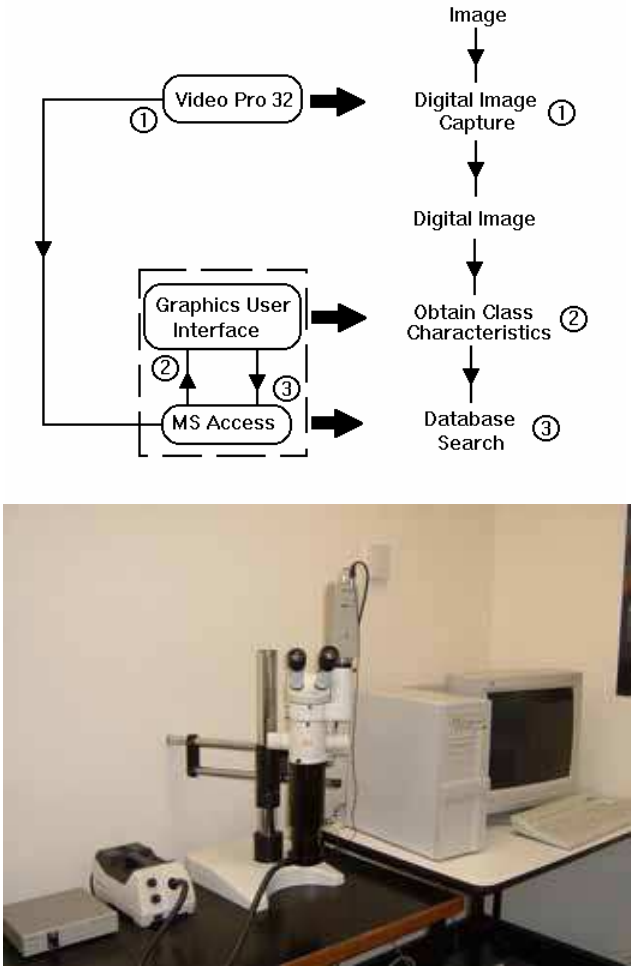

Fig. 20. FIREBALL structural schematic diagram and a photo of hardware.

only. FIREBALL is a tool that the ballistics expert can use to narrow down their field of search quickly and easily.

The FIREBALL system is comprised of image capturing software, custom designed graphics user interface (GUI) and Microsoft Access relational database (See Fig. 20).

Step 1 in the above figure is the image capture process. This sub-process is external to the FIREBALL database; therefore it is seen separate user interface. Step 2 is the GUI process of obtaining class characteristics. The GUI is custom software implemented separately to MS

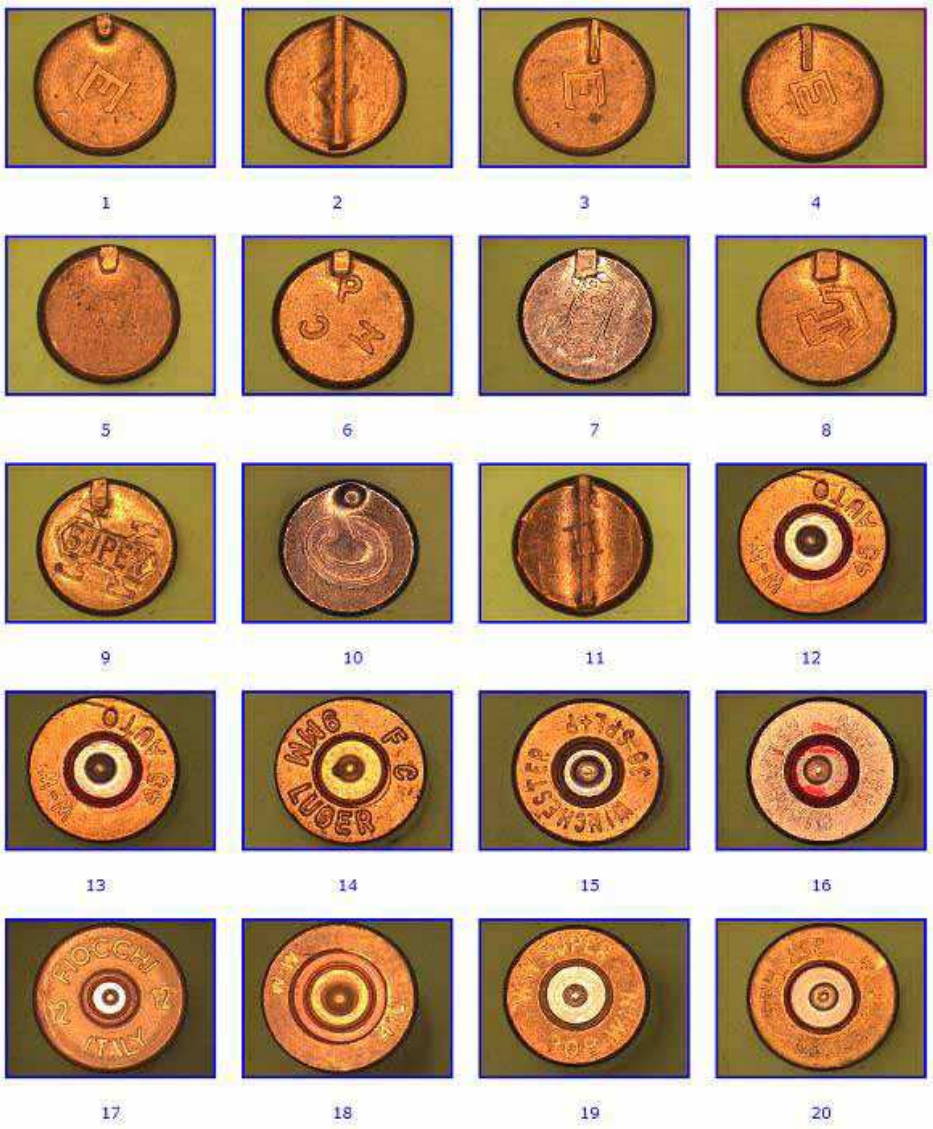

Fig. 21. Captured cartridge case images

Access; but to the end user the GUI software appears to be part of the database package. This is due to the GUI software being initiated and controlled from the database itself. The database search is implemented when control is returned to the database (ie. step 3). Fig. 21 shows some of acquired images of cartridge case heads in our database.

6. Web-based image processing and visualization

To overcome the limit and inconveience in infromation sharing arround the country, we are moving the system on-line. Applications have been developed to query the image database and display results on-line.

The original MS Acess database has be migrated to Oracle database to facilitate the database security and scalability. Since image data from all states wil be stored in this central database, MS Access may not be able to accomendate the amount of the data and the on-line transactions.

After migration, the image data are stored in an Oracle database as LOB datatype, which can store unstructured data and is optimised for large amounts of such data. Oracle provides a uniform way of accessing large unstructured data within the database or outside. We employ Oracle Objects for OLE (OO4O) and ASP for client to access the data including image data stored in BLOBs.

Fig. 22 shows the web interface for clients to query, search, and update the database.

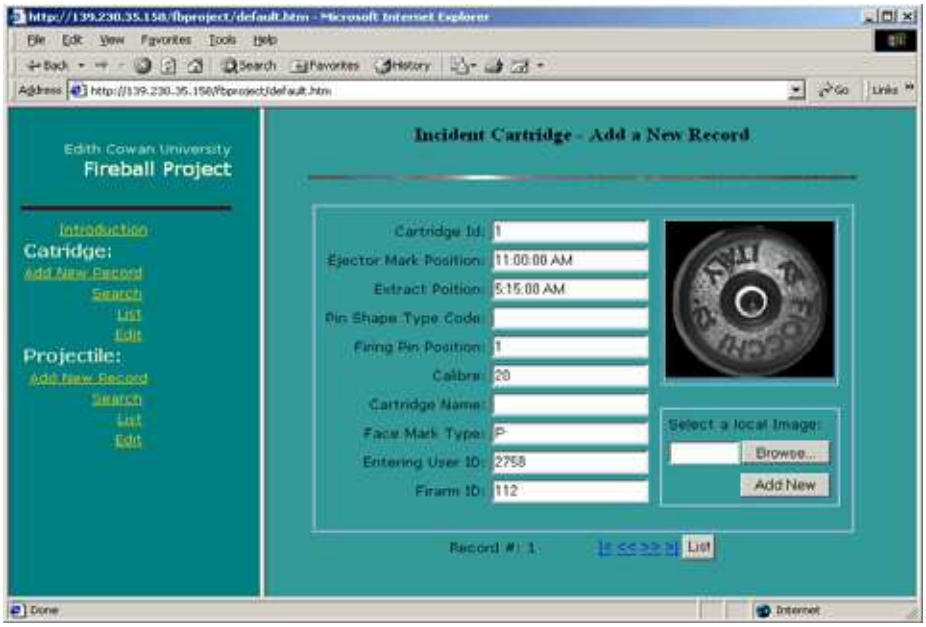

Fig. 22. Web Interface of the Fireball on-line system

The database query uses Oracle *OraDynaset* object that permits browsing and updating of data created from a *SQL SELECT* statement. An *OraDynaset* object represents the result set of a SQL SELECT query. It is essentially a client-side scrollable and updatable cursor that allows for browsing the set of rows generated by the query it executes.

This object provides transparent mirroring of database operations, such as updates. When data is updated via the Update method, the local mirror image of the query is updated so that the data appears to have been changed without reevaluating the query. The same procedure is used automatically when records are added to the *Dynaset*. Integrity checking is performed to ensure that the mirrored image of the data always matches the actual data present on the Oracle database.

To display the image on the Web retrieved from the database, we may use HTML tag <img src=location/ filename>.

However, the image data is actually stored in the database instead of a file. To overcome this burden, we use the method provided by ASP, *request.binaryWrite()* method. First, we compiled a ASP code to retrieve the image data from the database and write the image data as binary using *request.binarywrite()* to the web form to display the image. The cartridge case image shown in figure 3 is obtained in this way.

In general, the acquired image shows randomises in orientation, position and noise in the background. It is necessary to reduce the background noise and normalise the orientation, position and size of the image. If these simple image processing can be done on-line, that will bring much convenience.

We used ActiveX control techniques to realise the on-line image processing. The client retrieves the image data from the server database to the client browser. After processing, the image data is saved back to the database.

The first step of the image pre-processing is to find the cartridge case area in the image. Because of the good illumination and focusing, the acquired image has higher brightness in the cartridge case area than that in the rest. There is a clear edge around the cartridge case area. The edge detection should be an efficient way to detect cartridge case.

The proposed method employs Sobel Edge Operator [31] for detecting edges. At each point in the image a vertical slope and a horizontal slope are calculated. The maximum value of the two slopes is taken as the output value of that pixel. A threshold was chosen according to the average slope of the edge magnitude to eject noise edges. Fig. 23 shows the edges detected using Sobel edge operator. Strong edges are obvious. The outside circular edge defines the cartridge case area.

The feature extraction is performed based upon the result of the edge detection. Since the bottom of the cartridge case appears as a large circle, after edge detection, we use "direct least squares fitting of ellipses" [32] to fit the cartridge case edge data set.

This fitting algorithm provides an efficient method for fitting ellipses to scattered data. It solves the problem naturally by a generalized eigensystem and is extremely robust and computationally efficient. It should be possible to use the same algorithm for the active control in our proposed automatic image acquisition system.

After extracting the cartridge case area, we can manipulate the image, such as cleaning the background, centralising and rotating the image. These can all be done by clicking buttons in a Web browser.

Suppose the centre of the cartridge case and that of the image are (X_c, Y_c) and (X_i, Y_i), the spatial transformation of

$$\begin{cases} x' = x + X_i - X_c \\ y' = y + Y_i - Y_c \end{cases}$$

will take the cartridge to the center of the image. Figure 24 and 25 show the cartridge case image before and after centralising.

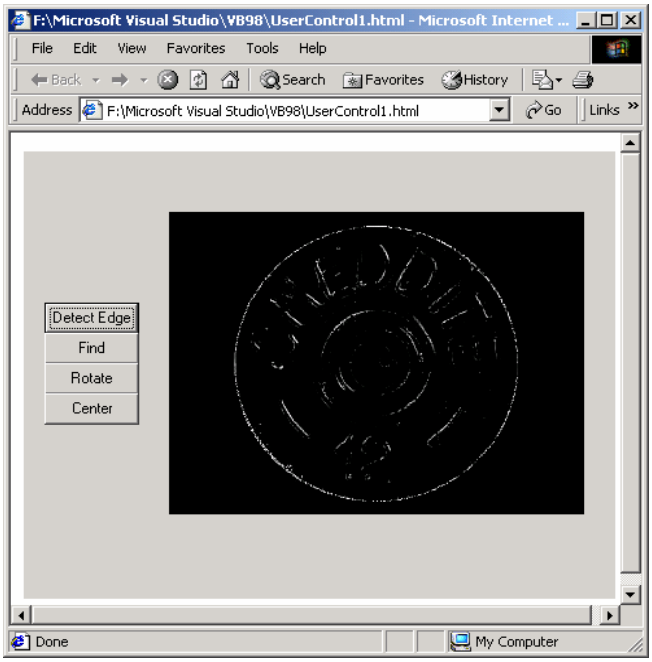

Fig. 23. Edges detected by Canny edge detection.

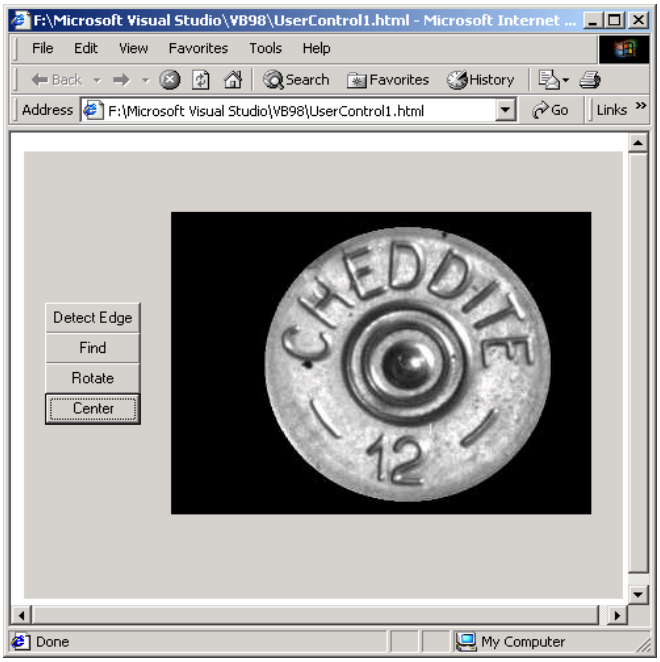

Fig. 24. The original Image

Fig. 25. The image after moving cartridge case to the center

7. Discussion and conclusion

Firearm identification is an intensive and time-consuming process that requires physical interpretation of forensic ballistics evidence. Especially as the level of violent crime involving firearms escalates, the number of firearms to be identified accumulates dramatically. The demand for an automatic firearm identification system arises.

This chapter proposes a new, analytic system for automatic firearm identification based on the cartridge and projectile specimens. Not only do we present an approach for capturing and storing the surface image of the spent projectiles at high resolution using line-scan imaging technique for the projectiles database, but we also present a novel and effective FFT-based analysis technique for analyzing and identifying the projectiles. This system can make a significant contribution towards the efficient and precise analysis of firearm identification based on projectile ballistics. The study demonstrates that different types of land and groove marks generated by different guns have distinctive surface textures, and spectral analysis can be used to measure and identify these textures effectively. Never have we seen before, a method such as this, that can study line-scanned images of projectile specimens so effectively. The method can overcome the difficulties involved with descriptions in the normal spatial domain in identifying texture features formed by land and groove marks on the surface of projectiles. In recent years the Hough transform and the related Radon transform have received much attention. These two transforms are able to transform two dimensional images with lines into a domain of possible line parameters, where each line in the image will give a peak positioned at the corresponding line

parameters. This has lead to many line detection applications within image processing. As the most features we are interested in from a line-scan image of the fired projectile are composed of various lines, it is possible to apply those transforms to the projectile image analysis. In the next step of our experiments we will investigate the potentials of those transforms for firearm identification.

A hierarchical neural network is used to create a firearm identification system based on cartridge case images. We focus on the cartridge case identification of rim-fire mechanism. Experiments show that the model proposed has high performance and robustness by integrating two levels; Self-Organizing Feature Map (SOFM) neural networks and the decision-making strategy.

A prototype of Web based cartridge case image database has been developed. The demonstration of querying and visualising the image data from the database on-line was successful. The proposed on-line image processing worked fine for cartridge case images.

By moving Fireball system on-line we can have following advantages:

- Real time input and update – enable input and update information to a central database quickly.
- Better data sharing – Enable users to obtain information from the latest resources in the central database.
- Easier management – Enable information to be stored in a central database that is easier to manage than many different copies stored on local PCs in various locations.

Some disadvantages are:

- The information retrieval may be slower, due to the transmission from Internet instead of retrieving data locally.
- Information security becomes a vital issue.

The significance of this research lies in the opportunity to produce the next generation of forensic ballistics digital information imaging systems for the identification of firearms. The automated imaging systems will have the capacity to provide class characteristic information directly to the firearms examiners and can significantly reduce the analytical effort needed for identification of firearms associated with ballistics specimens.

The research is innovative as it broadly extends the range of physical, optical, and photonic techniques for future examination, analysis, and comparison of test and crime scene ballistics specimens for positive identification. The traditional approach to forensic ballistics identification has essentially remained unchanged for the past century. However, forensic laboratories and Police Services now require a quantum step in precision of measurement, and speed of analysis for forensic policing. The research introduces the opportunity to explore new and innovative approaches to the examination of the surfaces of ballistics specimens in order to detect the individual markings and class characteristics that link the specimen to a particular weapon.

In firearm identification practice there are many practical difficulties. For instance the pattern of striations on a projectile are a function of an individual weapon which itself may be changed by wear, damage, oxidation and or building up of contaminants associated with the repeated use. One of solutions to overcome those difficulties is to introduce as many identifiers as we can in order to increase the reliability of the firearm identification system. Just like the human identification with fingerprints, sometimes only using one finger may result in false output although the fingerprint used is unique. By identifying more than one fingerprint (up to ten fingers) from the same person will assure the success. For the time

being, more than 30 different identifiers (such as make, model, brand, and type of the weapon; and shape, size, and position of marks on the specimen) are used in firearm identification. The FFT approach with the information on the frequency domain adds more identifiers to the collection of projectile features. In particularly with deformed projectile specimens routinely examined by ballisticians the FFT approach can still reveal the features of the markings created by weapon based on the spectrum analysis.

The research is also innovative in placing the development of optical and photonic techniques in the context of forensic science. The bench mark for forensic ballistics imaging has been set by the commercial products of IBIS and Drugfire, and the ECU Fireball imaging system. The research has markedly extended the optical and photonic physical methods of analysis of minute markings on the surfaces of forensic specimens.

For the future research the precise measurement of these features through imaging analyses will allow discrimination between the properties of the class characteristics and individual characteristics to identify the types of weapons. The development of multi-dimensional cluster analysis models for forensic ballistics specimens will identify the type of weapons that produced these ballistics specimens through intelligent imaging. Then the matching of metrics from line-scan and profilometry will allow identification of the weapon. Thus, by mapping the crime scene specimen to the multi-dimensional ballistics data, it will be possible to provide a rapid analysis of the involvement of the firearm. The potential to reduce the labour intensive activity of traditional ballistics identification provides the opportunity for rapid response in forensic ballistics analyses. Also the opportunity will be presented for better crime detection rates by police at crime scenes.

Experiments discussed in this chapter are performed on images by 16 various weapons only. Some more detailed experiments on features of various guns of the same kind and same make will be carried out in the next step of the research.

The need for intelligence applied to high resolution digital images systems for image processing is considerable, realizing the intensive nature of comparator microscope identification of forensic ballistics specimens. The future research will determine the optimum optical conditions for imaging ballistics specimens for comparison crime scene and test specimens.

In terms of cartridge case images, our main focus was on the consideration of rim-firing pin mark identification. Through the use of a hierarchical neural network model, this study investigated a system for identifying the firing pin marks of cartridge case images. The identification model in our study incorporates the combination of location and identification of firing pin marks of cartridge case images into one stage. It shows that the model proposed has high performance and robustness for real testing patterns.

Through further processing, such as the more efficient and precise identification of cartridge cases by combination with several characteristics on cartridge case images, the efficiency of this system will also make a significant contribution towards the efficient and precise identification of ballistics specimens.

8. References

[1] C.L. Smith, and J.M. Cross, (1995): Optical Imaging Techniques for Ballistics Specimens to Identify Firearms. Proceedings of the 29th Annual 1995 International Carnahan Conference on Security Technology, pp. 275-289, Oct. 1995, England.

[2] Smith, CL. (2001a). Profile measurements as a technique for forensic ballistics identification. Proceedings of 5th Australian Security Research Symposium, July, Perth, Western Australia, 153-162.

[3] Smith, C.L. (2002). Linescan imaging of ballistics projectile markings for identification. Proceedings of IEEE 36th Annual 2002 International Carnahan Conference on Security Technology, 216-222. Altantic City.

[4] Evans, JPO, Smith, CL and Robinson, M. (2004). Validiation of the linescan imaging technique for imaging cylindrical forensic ballistics specimens. American Firearm and Toolmark Examiners Journal. In press.

[5] Nichols, RG 1997. Firearm and toolmark identification criteria: A review of the literature. *Journal of Forensic Science*, 42(30, 466-474.

[6] Bunch, SG 2000. Consecutive matching striation criteria: A general critique. *Journal of Forensic Science*, 45(5), 955-962.

[7] Bonfanti, MS and Ghauharali, RJ 2000. Visualisation by confocal microscopy of traces on bullets and cartridge cases. *Science and Justice*, 40(40, 241-256.

[8] Springer, E. 1995. Toolmark examinations – A review of its development in the literature. Journal of Forensic Sciences, 40(6), 964-968.

[9] Smith, C.L. (1997). Fireball: A forensic ballistics imaging system. Proceedings of IEEE 31st Annual International Carnahan Conference on Security Technology, October, Canberra, Australia, 64-70.

[10] R. Saferstein (ED), (1988) Forensic Science Handbook: Volume 2. Englewood Cliffs: Prentice Hall, 1988.

[11] G.Burrard, (1951): Identification of Firearms and Forensic Ballistics. London: Herbert Jenkins,1951.

[12] Li, D.G. and Watson, A.C. (1998). Ballistics firearms identification based on images of cartridge case and projectile. Proceedings of 1998 SPIE Enabling Technologies for Law Enforcement and Security Symposium, Boston, USA, November 3-5.

[13] C.L. Smith, J.M. Cross, and G.J. Variyan, (1995): FIREBALL: An Interactive Database for the Forensic Ballistic Identification of Firearms. Research Report, Australian Institute of Security and Applied Technology, Edith Cowan University, Western Australia, 1995.

[14] Le-Ping Xin, (2000): A Cartridge Identification System for Firearm Authentication, Signal Processing Proceedings, 2000. WCCC_ICSP 2000. 5th International Conference on Volume: 2, P1405-1408.

[15] Chenyuan Kou, Cheng-Tan Tung and H. C. FU, (1994): FISOFM: Firearms Identification based on SOFM Model of Neural Network, Security Technology, 1994. Proceedings. Institute of Electrical and Electronics Engineers 28th Annual 1994 International Carnahan Conference on , 12-14 Oct. Pages: 120-125.

[16] Zographos, A., Robinson, M., Evans, J.P.O. and Smith, C.L. (1997). Ballistics identification using line-scan imaging techniques. Proceedings of IEEE International Carnahan Conference on Security Technology, Canberra, Australia.

[17] C.L. Smith, Robinson, M. and Evans, P.: (2000): Line-scan Imaging for the positive identification of ballistics, 2000. IEEE International Carnahan Conference on Security Technology, 269-275. 2000.

[18] Kingslake, R., Optics in Photography. SPIE Optical Engineering Press. Bellingham, Washington, USA, 1992.

[19] Evans J.P.O., Zhu C and Robinson M.: Line-scan imaging using an area array camera, The 5th Int. Conf on Control, Automation, Robotics and Vision, pp. 1471-1475, Singapore, 1998, ISBN 981-04-0318-6.
[20] Patent number EP1418767 Line-scan imaging system in 3-D.
[21] Jun Kong, D. G. Li., A. C. Watson: A Firearm Identification System Based on Neural Network, AI 2003, Lecture Notes in Artificial Intelligence, 315-326, 2003, Springer.
[22] Rafael C. Gonzalez, Richard E. Woods: Digital Image Processing, Second Edition, Beijing: Publishing House of Electronics Industry, 2002, 7, 519-566.
[23] Pitas I.: Digital image processing algorithms, Prentice Hall, ISBN 0-13-145814-0, 1993
[24] Chenyuan Kou, Cheng-Tan Tung and H. C. FU, (1994) "FISOFM: Firearms Identification based on SOFM Model of Neural Network", Security Technology, 1994. Proceedings. Institute of Electrical and Electronics Engineers 28th Annual 1994 International Carnahan Conference on , 12-14 Oct. Pages: 120-125.
[25] T. Kohonen, (1990) "Self-organising Maps", Springer, Berlin, 1995, The self-organising Maps, Proc. IEEE 78 (9) (1990) 1464-1480.
[26] S.B. Cho, "Pattern Recognition with Neural Networks Combined by Genetic Algorithm", Fuzzy Set and System 103(1999) 339-347.
[27] T.M. Ha, H. Bunke, "Off-line Handwritten Numeral Recognition by Perturbation Method", IEEE Trans. Pattern Anal. Mach.Intell. 19(5) (1997)535 -539.
[28] P.N. Suganthan, "Structure Adaptive Multilayer Overlapped SOMs with Partial Supervision for Handprinted Digit Classification ", Proceedings of International Joint Conference on Neural Networks, WCCI'98, Alaska, May 1998.
[29] T. Kohonen, Tutorial Notes, (1993) International Symposium on Artificial Neural Networks, pp. 9-15, Dec.20-22, 1993.
[30] Rafael C. Gonzalez, Richard E. Woods, Digital Image Processing, Second Edition, Beijing: Publishing House of Electronics Industry, 2002, 7, 519-566.
[31] k. R. Castleman *Digital Image Processing, 1996, Prentice Hall, Inc.*
[32] A. W. Fitzgibbon, M. Pilu and R. B. Fisher, *"Direct least squares fitting of ellipses",* in Proceedings of International Conference on Pattern Recognition, Vienna, 1996

Image Processing

Edited by Yung-Sheng Chen

ISBN 978-953-307-026-1
Hard cover, 516 pages
Publisher InTech
Published online 01, December, 2009
Published in print edition December, 2009

There are six sections in this book. The first section presents basic image processing techniques, such as image acquisition, storage, retrieval, transformation, filtering, and parallel computing. Then, some applications, such as road sign recognition, air quality monitoring, remote sensed image analysis, and diagnosis of industrial parts are considered. Subsequently, the application of image processing for the special eye examination and a newly three-dimensional digital camera are introduced. On the other hand, the section of medical imaging will show the applications of nuclear imaging, ultrasound imaging, and biology. The section of neural fuzzy presents the topics of image recognition, self-learning, image restoration, as well as evolutionary. The final section will show how to implement the hardware design based on the SoC or FPGA to accelerate image processing.

InTech Europe
University Campus STeP Ri
Slavka Krautzeka 83/A
51000 Rijeka, Croatia
Phone: +385 (51) 770 447
Fax: +385 (51) 686 166
www.intechopen.com

InTech China
Unit 405, Office Block, Hotel Equatorial Shanghai
No.65, Yan An Road (West), Shanghai, 200040, China
中国上海市延安西路65号上海国际贵都大饭店办公楼405单元
Phone: +86-21-62489820
Fax: +86-21-62489821